Recombination activity of contaminated dislocations in silicon: A model describing electron-beam-induced current contrast behavior

V. Kveder,[1,*] M. Kittler,[2] and W. Schröter[1]

[1]*IV. Physikalisches Institut, Universität Göttingen, Bunsenstrasse 13-15, D-37073, Göttingen, Germany*
[2]*IHP, Im Technologiepark 25, D-15236 Frankfurt(Oder), Germany*
(Received 15 September 2000; published 2 March 2001)

Existing experimental data give many evidences that the recombination rate of minority charge carriers at dislocations in silicon depends strongly on dislocation decoration by transition metal impurities. Here, we present a model that allows a quantitative description of the recombination of minority carriers at decorated dislocations. It assumes that shallow dislocation bands, induced by the strain field, and deep electronic levels, caused by impurity atoms, which have segregated at the dislocation, or by core defects, can exchange electrons and holes. As a consequence, the recombination of carriers captured at dislocation bands can be drastically enhanced by the presence of even small concentrations of impurity atoms at the dislocation core. The model allows us not only to explain experimentally observed dependences of the recombination rate on temperature and excitation level, but also to estimate the concentration of deep level impurities at dislocations.

I. INTRODUCTION

Dislocations are responsible for the plastic behavior of crystalline materials, but they may also significantly influence the electrical properties, especially of semiconductors. During material growth or technological processing stress release easily generates dislocations, and in semiconductors these have been found to impact device performance. Therefore, in the case of silicon integrated circuits, major efforts have been and are still made to avoid dislocation generation. However, the development of some low-cost multicrystalline silicon materials like cast silicon or silicon ribbons for photo voltaic applications, demands alternative strategies of defect engineering, since in these materials dislocations are inherent.

One parameter that is directly related to the solar cell efficiency and which is strongly affected by dislocations, is the minority carrier lifetime τ_{minor}. To preliminary experimental evidence, not the dislocation core states or core defect states, but some metallic impurities like Fe, Ni, and Cu segregated or precipitated at the dislocation, induce the effect of dislocations on τ_{minor}. These impurities are well known in silicon microelectronics technology. Their ubiquitous presence and their unusually high diffusivities[1,2] have again and again created severe problems for the device performance.

Several techniques to study the recombination activity of dislocations are at hand. Some of these, such as scanning deep level transient spectroscopy, scanning photoluminescence, infrared-beam-induced current, and electron-beam-induced current (EBIC) are unique among the electrical characterization methods with respect to a spatial resolution, sufficient to measure at single dislocations. The most widely used among these techniques is EBIC. In EBIC, the variation of the induced current I at a Schottky contact resulting from nonequilibrium electrons and holes generated by the electron beam, is measured, while the specimen area of interest is scanned. The values of I at the dislocation, I_{disl}, and away from it, I_0, are used to define the contrast C_{disl} $=(I_0-I_{disl})/I_0$ of single dislocations. The measured characteristics of dislocations comprise $C_{disl}(T,I_{beam})$ where T is the specimen temperature and I_{beam} is the beam current of the electron probe.

Numerous experimental investigations[3–10] of the effect of metallic impurities on C_{disl} have established four classes of $C_{disl}(T,I_{beam})$ dependences ranging from ''pure'' dislocations with rather small contrasts observable only at low temperatures (around 50–80 K) to dislocations decorated by precipitates with very strong contrast slowly increasing with temperature. It has been shown that large silicide precipitates of Cu and Ni may act as internal Schottky contacts, which presumably allows us to account for $C_{disl}(T,I_{beam})$ of the last class.[11,12] However, the interaction of metallic impurities with dislocations in the preprecipitation stage and the resulting coupling of their electronic states with those at the dislocation itself have not been tackled so far by any of the existing recombination models for dislocations.

As we will show in this paper, there is a strong coupling between deep impurity levels and one-dimensional bands, which are split off from the valence- and conduction-band edges by the action of the dislocation deformation potential. A fit of our model to measured $C_{disl}(T,I_{beam})$ data allows us to determine three free parameters of the model, so that the physical relevance of the model can be checked through the consistency of these parameters with what is expected from data obtained by other experimental techniques. One of the parameters is a measure of the concentration of metallic impurities at the dislocation, so that we are in the position to discuss the physical and technological implications of metallic impurity segregation at dislocations.

The paper is composed as follows: in Sec. II we shall briefly discuss some typical experimental data $C_{disl}(T)$ obtained for dislocations with different levels of impurity decoration and their common features. In Sec. III A we shall make some introductory remarks explaining the main idea of the proposed model and also discuss the assumptions we will use. In Secs. III B–III F the equations, used for model calcu-
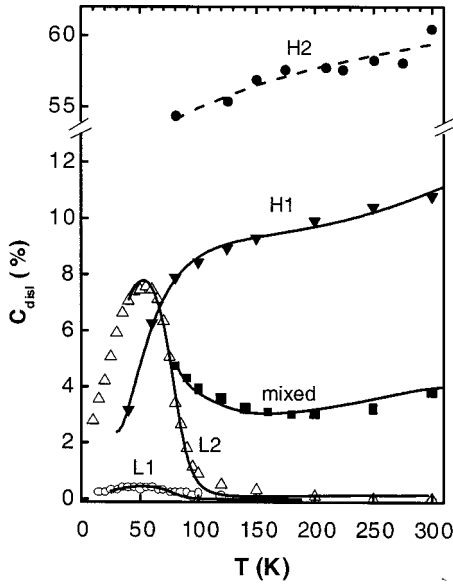
FIG. 1. Temperature dependences of the EBIC contrast $C_{disl}(T)$ of dislocations in Si. Different types of behavior reflect the effect of different concentration of deep level impurities at dislocations. Points are experimental data, solid curves are calculated using our model.

lations will be presented, as well as estimations for some parameters of the model, which are necessary to reduce a number of fit parameters. In Sec. IV we present results of model calculations and their comparison with experimental data, and finally, in Sec. V A we discuss previous models for recombination at dislocations. In Sec. V B we give a summary.

II. EXPERIMENTAL OBSERVATIONS

It was found that dislocations in different samples often exhibit significantly different EBIC contrast behavior $C_{disl}(T)$.[3-10] Figure 1 shows typical examples of experimental $C_{disl}(T)$ data measured for dislocations in different samples, but similar experimental conditions. Points in Fig. 1 show the experimental results, while the solid curves have been calculated using our model, presented in Sec. III. Different types of $C_{disl}(T)$ behavior can be distinguished:[3,4] Types $L1$ and $L2$ are characterized by a quite small contrast of dislocations at room temperature and by increasing contrast with decreasing temperature, exhibiting a maximum between 50 and 90 K. The contrast value in the maximum increases drastically with increasing decoration level of dislocations[3,4,9,13] from 0.5% for ''clean'' dislocations, up to 10% for dislocations contaminated by impurities. Types $H1$ and $H2$ exhibit recombination activity over the whole temperature range and the $C_{disl}(T)$ increases with increasing temperature. There is also a mixed type of behavior that looks like a superposition of types L and H.[14,15]

The contrast of dislocations at 300 K varies from type $L1$ to type $H2$ by more than a factor of 500. Only in the case of type $H2$, with a contrast of more than 30–40 %, silicide precipitates have been found to be connected to the dislocations.

This case is out of the scope of our model.

It has been found that with increasing metal contamination the $C_{disl}(T)$ behavior of dislocations changes in the sequence: type $L1 \rightarrow$ type $L2 \rightarrow$ mixed type $\rightarrow$ type $H1 \rightarrow$ type $H2$. The type of the metal (Cu, Ni, Fe, or Au) decorating the dislocation, was found not to be important for $C_{disl}(T)$ characteristics. Experiments with hydrogenation[4] and phosphorus diffusion gettering[16] have shown that both passivation and gettering of impurities decorating dislocations, change the $C_{disl}(T)$ behavior in a reverse sequence, from type $H1$ to type $L2$ to $L1$, so that the contrast value in the maximum can be reduced to the level of 1.5–2% .

III. THE MODEL

A. Introductory

1. Dislocation recombination strength and EBIC contrast

Using an analytical procedure developed by Donolato,[17] the EBIC contrast C_{disl} may be evaluated from the recombination strength Γ of the dislocation, which is defined as the recombination rate R_T of minority carriers at the dislocation divided by the excess minority carrier density p_{SCR} at the border of a space charge region around the charged dislocation and their diffusivity D: $\Gamma = R_T/(D\,p_{SCR})$. In the linear contrast model one has $C_{disl} = B\Gamma$ where B is dependent on the electron beam energy, on τ_{minor} or minority-carrier diffusion length of the material and on the distance d of the dislocation from the Schottky contact. Usually, the diffusion length of free minority carriers is much larger than a penetration depth of electron beam d_e. In that case, the EBIC contrast depends only on recombination strength Γ and on the depth d of the dislocation below the Schottky contact. According to Ref. 18, the contrast has a maximal value C_{max} when $d \approx d_e/1.2$, and this value is approximately equal to

$$C_{max} \approx 0.2\Gamma/[1 + (\Gamma/2\pi)\ln(2d/L_{SCR})]. \tag{1}$$

Here, L_{SCR} is the radius of the space charge region around the dislocation. The correction term $(\Gamma/2\pi)\ln(2d/L_{SCR})$ in Eq. (1) takes into account that p_{SCR} is smaller than the average hole concentration p in a generation volume of an electron beam far from dislocation due to diffusion limitation:

$$p_{SCR} \approx p - [R_T/(2\pi D)]\ln(2d/L_{SCR}). \tag{2}$$

Therefore, the problem to be solved is to calculate the recombination rate R_T of minority carriers at the dislocation.

2. Energy bands at dislocations

Theoretical investigations have shown that straight 60° dislocations, which are dissociated into 30° and 90° partial dislocations with a stacking fault ribbon between them, have reconstructed cores and are not associated with any deep one-dimensional bands in the band gap of silicon.[19] However, theory has found relatively shallow bands to be associated with the strain field of the dissociated dislocation. An empty one-dimensional (1D) band D_e and a full one D_h have been predicted to split off from the conduction band and valence band edge, respectively. The radii of the wave func-
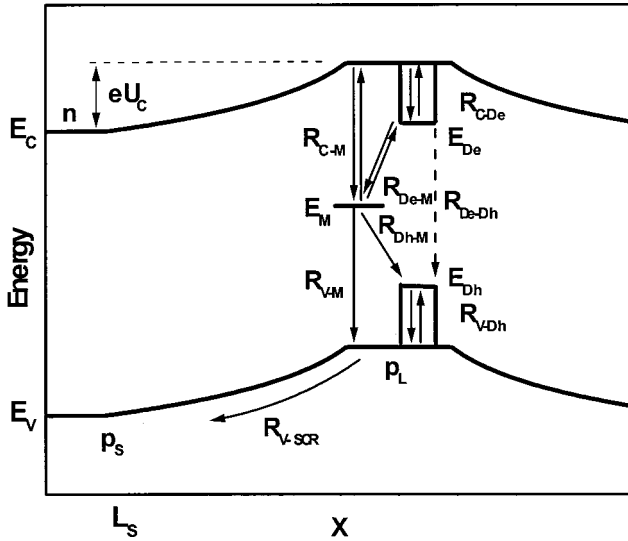
FIG. 2. Charge carrier recombination on dislocations. For clean dislocations the recombination rate is determined by direct recombination of electrons and holes captured by 1D dislocation bands E_{De}, E_{Dh} (channel R_{De-Dh}). In presence of deep centers with the energy level E_M, the carriers captured to 1D bands can recombine by transitions R_{De-M}, R_{Dh-M} via this deep level.

tions of electrons and holes captured to the bands D_e and D_h are larger than the dislocation core and their centers of gravity are outside the dislocation core. To distinguish between free charge carriers around a charged dislocation and those bound to D_e or D_h, we define an extended core region of radius $L_d \ll L_{SCR}$. Recently it has been shown,[20] that small line charges of the dislocation, which are presumably realized in many EBIC investigations (see Sec. III B), lead to a rigid shift of all states inside the extended core region.

In the analysis and interpretation of experimental data, those dislocation bands D_e and D_h have been related to various physical phenomena: microwave conductance,[21–23] electric-dipole spin resonance,[24] and photoluminescence.[25–27] From those results, consistent values for the position of the edges of the one-dimensional (1D) bands at $E_C - E_{De} \approx E_{Dh} - E_V \approx 70-80$ meV have been obtained.

In addition to the shallow bands D_e and D_h, dislocations can have deep localized electronic states, originating in core defects, like dangling bonds in reconstruction solitons etc., or from fast diffusing impurity atoms (like Cu, Fe, Ni, etc.) segregated in the dislocation core. We note that electronic energy levels and capture cross sections of impurities incorporated into dislocation cores may differ from the respective values of the same impurities in the bulk. In contrast to the 1D bands D_e and D_h, that are inherent to dislocations, the concentration of deep electronic states, related to core defects and impurities, depends strongly on the sample history and can vary in a wide range.

The new feature of our model (see Fig. 2) has evolved from comparison of type $L1$ and type $L2$ $C_{disl}(T)$ curves. Type $L1$ has been ascribed to ``clean'' dislocations with a very small concentration of deep electronic states at dislocations, type $L2$ to dislocations slightly decorated by metal impurities with deep electronic states. On their high-

temperature sides, the $C_{disl}(T)$ curves of $L1$ and $L2$-type decrease exponentially with temperature. The activation energies are found for all $C_{disl}(T)$ curves of type $L1$ and $L2$ to be between 70–80 meV, both in n-type and p-type silicon. Therefore, we suggest that this decay of $C_{disl}(T)$ is caused by the thermally activated emission of electrons and holes from the one-dimensional energy bands D_e and D_h. Hence, the capture of charge carriers at those bands must be the first step in the electron-hole recombination process.

According to the experimental data (presented in Sec. II) the contrast of clean dislocations is very small, less or about 0.5%. We suppose that the recombination rate caused by direct transitions between one-dimensional (1D) bands D_e and D_h is quite small in silicon. This is in agreement with theoretical results obtained by Farvacque,[28] who considered the electron-hole recombination at dislocations as the sequence of the cascade captures of electrons by D_e of holes by D_h, and the radiative electron transition between D_e and D_h. The rate of the last step compared to that of the first two steps has been found to be large in direct semiconductors like GaAs and very small in indirect semiconductors like Si.

On the other hand, the EBIC contrast of $L2$ type is 20–30 times larger than for clean dislocations (type $L1$). How can the presence of deep levels at dislocations enhance so strongly the recombination of electrons and holes, captured by the dislocation energy bands? To account for this dramatic increase, we assume in our model that the recombination of charge carriers captured by the 1D bands may occur not only by electronic transitions between those bands, but also by transitions via deep levels. These levels may originate in impurity atoms or core defects spatially located near to the dislocation core so that overlap of their wave functions with those of the bands D_e and D_h initiates this new recombination channel.

B. Kinetic equations

We consider n-type silicon with shallow donors of concentration N_d. Holes will be minority carriers and dislocations will be negatively charged. A similar treatment would hold for positively charged dislocations in p-type Si.

Since a general treatment of carrier recombination at dislocations is missing at present, we shall consider a simplified model adjusted to the conditions under which EBIC is usually measured.

As mentioned above, the type of the metallic impurities investigated so far is not reflected in the measured $C_{disl}(T)$ data. Therefore, we consider only one deep acceptor level at $E_C - E_M$ of concentration N_M per unit dislocation length, either attracted by the elastic strain field of the dislocation or bound to its core.

In addition, we assume that the electric charge eN_{tot} of the dislocation under EBIC conditions is small enough to neglect the modification of the wave functions of the 1D bands D_e and D_h and some other corrections that can become important at high dislocation charges. We have checked by numerical simulation and comparison of our model with the

experimental data that this assumption yields a consistent description of recombination if the experimental conditions are chosen so that:

(1) The temperature $T > 40$ K and the dopant concentration $N_d < 10^{16}$ cm^{-3}. Note that in this case, coupling of minority carriers to excitons as well as free carriers degeneration can be neglected. To calculate the concentration n of free electrons from N_d we use standard formulas from Refs. 29 and 30.

(2) The free hole concentration p (minority carriers) under electron-beam excitation reaches the condition $p/n > 10^{-4}$. In EBIC measurements, the concentration of minority carriers p is usually higher than 10^{12} cm^{-3} so that the condition holds since we have already assumed $N_d < 10^{16}$ cm^{-3}.

(3) The space-charge regions of charged dislocations are not overlapping. This condition is valid since the distance between neighboring dislocations has to be larger than 1 μm due to the limited spatial resolution of EBIC.

To formulate rate equations for our model, we note that each of the shallow dislocation 1D bands exchanges electrons or holes with the conduction or valence band, respectively, and with the deep levels of metal atoms or core defects, whereas the deep levels exchange charge carriers with the two dislocation bands and also with the conduction and valence band. In addition, there is a small direct e-h recombination between D_e amd D_h.

Denoting by R_{ij}, the difference of capture and emission rate between states i and j, and making use of the notation introduced in Fig. 2 we obtain

$$dn_{De}/dt = R_{C\text{-}De} - R_{De\text{-}M} - R_{De\text{-}Dh} \qquad (3)$$

$$dp_{Dh}/dt = R_{V\text{-}Dh} - R_{Dh\text{-}M} - R_{De\text{-}Dh} \qquad (4)$$

$$dn_M/dt = R_{De\text{-}M} + R_{C\text{-}M} - R_{Dh\text{-}M} - R_{V\text{-}M}, \qquad (5)$$

where the n_{De} and p_{Dh} are the concentration of electrons and holes per unit dislocation length in the bands D_e and D_h with lower edges at $E_C - E_{De}$ and $E_V + E_{Dh}$, respectively, and n_M is the concentration of electrons (per unit dislocation length) captured by deep impurities at $E_C - E_M$.

The total recombination rate R_T of charge carriers at the dislocation is given by the sum $R_T = R_{Dh\text{-}M} + R_{V\text{-}M} + R_{De\text{-}Dh}$ and can be calculated by solving the set of Eqs. (3)–(5) for the stationary state $dn_{De}/dt = dp_{Dh}/dt = dn_M/dt = 0$.

C. Transitions between deep impurity or core defect levels and conduction or valence band

Dislocations are extended defects with a large number of electronic states, whose occupation generates a line charge $eN_{\text{tot}} = e(n_M + n_{De} - p_{Dh})$. The interaction of free charge carriers with this line charge results in significant modifications of electron and hole transitions to or from the dislocation,[31] which have been investigated in some detail in the literature and were taken into account also in all previous models describing recombination at dislocations (see Sec. V A).

Let us consider a negatively charged dislocation in n-type silicon. In this case, free-electron capture by deep metal or core defect acceptor levels is impeded by a capture barrier eU_C, so that

$$R_{C\text{-}M} = n\sigma_e v_{\text{the}}(N_M - n_M) \exp(-eU_C/kT)$$
$$- N_C \sigma_e v_{\text{the}} n_M \exp[-(E_C - E_M)/kT]. \qquad (6)$$

Here, σ_e is the capture cross section of the neutral impurity atom for electrons, $v_{\text{the}} \approx 1.17\,10^6 T^{1/2}$ cm/sec is the thermal velocity of electrons, and N_C is the effective density of states in the conduction band ($N_C \approx 5.44 \times 10^{15} T^{3/2}$ cm^{-3}). The first term describes the capture of free electrons by the acceptor level E_M, while the second term describes their thermal activated emission back to the conduction band.

Free hole capture is accelerated by the attractive potential of the negatively charged dislocation:

$$R_{V\text{-}M} = p_d v_{\text{thh}} \sigma_h n_M. \qquad (7)$$

Here, σ_h is the hole capture cross section of negatively charged impurity atoms segregated at the dislocation, $v_{\text{thh}} \approx 0.91\,10^6 T^{1/2}$ cm/sec is the hole thermal velocity, and p_d is the concentration of free holes at the boundary of the extended core region of the dislocation ($L = L_d$), inside which the bands D_e, D_h, and segregated metal impurities are localized. The thermal emission of holes is neglected since holes are captured by the negatively charged acceptors and immediately recombine with the electrons already present.

The capture barrier eU_C and the local density of holes p_d in the vicinity of the extended core region are parameters, which represent the effect of the dislocation line charge on the capture rates. Following Read,[32] the Coulomb potential $eU(L)$ of the total dislocation line charge eN_{tot} at a distance L, smaller than the screening radius L_{SCR}, can be approximated as

$$eU(L) \approx \beta N_{\text{tot}}[\ln(L_{\text{SCR}}/L) + 0.5(L^2/L_{\text{SCR}}^2) - 0.5], \quad (8)$$

where $\beta = e^2/(2\pi\varepsilon\varepsilon_0)$, ε is the dielectric constant and e is the electron charge. The screening radius L_{SCR} is approximately equal to $L_{\text{SCR}} = (N_{\text{tot}}/\pi N_c)^{1/2}$.

To estimate the electrostatic barrier for electron capture eU_C, we assume $L = L_d = 1/N_{\text{tot}}$ in Eq. 8. Since $L_d/L_{\text{SCR}} \ll 1$ (see Sec. III A) we have

$$eU_C \approx \beta N_{\text{tot}}\{\ln[N_{\text{tot}}^{3/2}/(\pi N_d)^{1/2}] - 0.5\}. \qquad (9)$$

Here, we have neglected a tunneling of electrons through the barrier and influence of deformation potential on the barrier height.[20]

Holes inside the space-charge region of the dislocation are treated under the assumption of small dislocation charges, made above, so that the influence of bound hole states on hole capture may be neglected. The confinement energy $E_{\text{conf}} \approx N_{\text{tot}}^2 h^2/(32m_h)$ is then less or about kT at least for the heavy holes ($m_h \approx 0.5m_0$), which can be considered in a classical approximation at least up to a distance of about $L_d = 1/N_{\text{tot}}$ from the dislocation core.

The recombination of holes at negatively charged dislocations occurs in a sequence of three steps:

(1) diffusion of holes from bulk region ($L \gg L_{SCR}$), where the hole density p under the e-beam generation of EBIC has adjusted unaffected by dislocations, to the border of the dislocation space-charge region, where $p_{SCR} = p(L_{SCR})$,

(2) capture by the space-charge region (rate R_{V-SCR}), yielding $p_d \approx p(L_d)$ for the density of free holes at the extended core region of the dislocation, and

(3) capture by the band D_h or by the negatively charged deep states E_M and then recombination with electrons captured at the dislocations (rate R_T, see Sec. III B).

When the rate of step (3), R_T, is much smaller than that of step (2), R_{V-SCR}, we obtain with the assumption of small dislocation line charges made above $p_d \approx p_{SCR} \exp(eU_C/kT)$.

With increasing concentration of deep acceptors at the dislocation, N_M, the recombination rate R_T will increase and might become comparable with R_{V-SCR}, so that the capture of free holes by the space-charge region of the dislocation intervenes. Carrier capture by attractive centers is a subject that has attracted a great deal of attention. The basic mechanism and first calculation of cross sections have been developed for gases[33,34] and then modified for the treatment of deep point defects in semiconductors.[35–37] Using these concepts, we shall estimate the capture radius L_C of dislocations in Sec. III F.

For given L_C, the local concentration p_d under steady state conditions can be estimated as

$$p_d \approx (p - KR_T) \exp(eU_C/(kT)), \tag{10}$$

where K is the coefficient given by

$$K = 1/(2L_C v_{thh}) + \ln(2d/L_{SCR})/(2\pi D). \tag{11}$$

The second term in Eq. (11) results from Eq. (2), which relates p_{SCR} to p.

D. Transitions between the dislocation bands and conduction or valence band

Capture of free electrons and holes by the 1D bands D_e and D_h, respectively, and their re-emission are considered as competitive processes to the direct recombination by deep acceptors in the extended core region of dislocations

$$R_{C-De} \approx S_{De} n (N_{De} - n_{De}) \exp(-eU_C/kT) - S_{De} N_C n_{De}$$
$$\times \exp[-(E_C - E_{De})/kT]. \tag{12}$$

Here, S_{De} is the capture coefficient and N_{De} is the number of states in the band D_e below the edge of conduction band E_C, n_{De} is the number of captured electrons, both taken per dislocation unit length. The two terms are obtained as approximations for $n_{De}/N_{De} \lesssim 0.3$ from an integral taken over the product of the emission rate, density of D_e states and Fermi occupation probability as a function of energy from E_C to $E_C - E_{De}$. They have to be replaced by the full integral expressions for $n_{De}/N_{De} \gtrsim 0.3$.

Capture of free holes by the shallow one-dimensional dislocation band D_h and their re-emission is written correspondingly

$$R_{V-Dh} \approx S_{Dh} p_d (N_{Dh} - p_{Dh}) - S_{Dh} N_V p_{Dh}$$
$$\times \exp[-(E_{Dh} - E_V)/kT], \tag{13}$$

where S_{Dh} and N_{Dh} have analogous meanings as for electrons and $N_V \approx 2.12 \times 10^{15} \, T^{3/2} \, cm^{-3}$ is the effective density of states in the valence band.

The number of states N_{De} and N_{Dh} can be estimated using the effective mass approximation:[38,39] $N_{De} = [8m_{De}(E_C - E_{De})]^{1/2}/h$ and $N_{Dh} = [8m_{Dh}(E_{Dh} - E_V)]^{1/2}/h$ where h is the Planck constant, and the effective masses in 1D bands may be taken from theoretical calculations as $m_{De} \approx 0.3m_0$ and $m_{Dh} \approx 0.5m_0$. m_0 denotes the free electron mass.

A theoretical treatment of the capture of holes by a 1D band at a negatively charged dislocation has been given by Sokolova.[40] The capture occurs by successive transitions between the states of the valence band and of the 1D band at the dislocation, and exhibits a certain similarity to the cascade capture of carriers by attractive point defects. The resultant capture coefficient is weakly temperature dependent (see Sec. III F).

E. Transitions between 1D bands and deep levels

The second step following the capture at the 1D bands is the recombination of the electrons captured at D_e and the holes captured at D_h, which occurs either by a direct electron transition from D_e to D_h, or via deep acceptor states M at E_M localized in the extended core region. The rate R_{De-M} for the transitions between band D_e and deep acceptor level M is given by

$$R_{De-M} \approx A_e v_{De} \{(N_M - n_M) n_{De} - n_M N_{De}$$
$$\times [kT/(E_C - E_{De})]^{1/2} \exp[-(E_{De} - E_M)/kT]\}. \tag{14}$$

Here, $v_{De} \approx (kT/m_{De})^{1/2}$ is a thermal velocity of electrons in the D_e band and A_e is a capture parameter describing the coupling between D_e states and M states and depending on the nature of the deep centers and their spatial location (see Sec. III F). The emission term is written in the approximation of low occupation of the 1D band (see Sec. III D). It can be shown that for $E_C - E_M > 0.2$ eV, this term becomes important only at high temperature, when the occupation of the 1D band is already very small.

The transitions of holes from the 1D band to negatively charged impurity atoms can be described by

$$R_{Dh-M} = A_h v_{Dh} n_M p_{Dh}, \tag{15}$$

where $v_{Dh} \approx (kT/m_{Dh})^{1/2}$ is the thermal velocity of holes in the 1D band and A_h is a capture parameter.

The recombination rate of 1D holes with 1D electrons is

$$R_{De-Dh} \approx A_{1D} n_{De} p_{Dh}, \tag{16}$$

where A_{1D} is a coefficient that can be estimated once from the experimentally measured EBIC contrast $C_{disl}(T)$ of clean dislocations. Since this contrast is very small, less than 0.5%,[3,4] in most cases the term R_{De-Dh} can be neglected, except for dislocations with a very small concentration of deep levels.

To calculate the recombination rate R_T and the contrast C_{disl} the set of Eqs. (3)–(5) has to be solved numerically for the stationary state $dn_{De}/dt = dp_{Dh}/dt = dn_M/dt = 0$, e.g., by using the standard globally convergent Newton method. The calculation of a contrast $C_{disl}(T)$ in the temperature range 40–350 K takes a few seconds at any personal computer, so that a fit to experimental EBIC data using, for example, the well-known Marquard algorithm can be easily performed.

F. Estimations of some parameters

A critical check of our model, proposed and developed in the previous sections, by comparison with available experimental EBIC data implies a careful look, which parameters of the model might be taken or estimated from independent experiments or theoretical calculations.

The depths E_{De} and E_{Dh} of 1D bands can be quite well estimated from independent measurements.[21–27] We shall use the value $E_C - E_{De} \approx E_{Dh} - E_V \approx 0.075$ eV.

The diffusion coefficient of free holes D is important for the calculation of the EBIC contrast from the recombination rate R_T. We estimate $D(T)$ from the mobility of holes μ_h in Si using the Einstein relation $D = \mu_h kT/e$. For $N_d < 10^{16}$ cm^{-3} and $T > 100$ K, the mobility is mainly controlled by phonon scattering: $\mu_h \approx \mu_{h-ph} \approx \mu_0(T/300)^{-2.2}$ where $\mu_0 \approx 480$ cm^2/Vs.[41,42] At low temperatures, carrier scattering by ionized impurities usually affects the mobility. This contribution has been estimated using standard expressions given in Refs. 29 and 30.

For the capture coefficients S_{De} and S_{Dh}, representing the carrier capture by the dislocation bands D_e and D_h, we take the theoretical values given by Sokolova:[40] $S_{De} = S_{De0}/T^{3/2}$ and $S_{Dh} = S_{Dh0}/T^{3/2}$ with $S_{De0} \approx S_{Dh0} \approx 2 \cdot 10^{-3}$ cm^3 K$^{3/2}$/s. We mention that Sokolova's results have been already integrated in previous models of carrier recombination at dislocations by Schröter,[43] Ourmazd,[44] and by Wilshaw and Booker.[45]

The capture of free holes by the space-charge region of the dislocation occurs in a series of inelastic scattering events between holes and acoustical phonons, each leading to a loss of energy of the order $(m_h s^2 E)^{1/2}$, (E is the kinetic energy of holes, s is the sound velocity), until the total loss brings the hole to a state with $E - eU(L) < 0$. According to previous investigations,[32,34] the capture radius can be estimated as the product of the radius L_T, defined by $eU(L_T) = kT$, with the probability for holes to lose the kinetic energy of about kT in the time it resides within the cylinder of radius L_T.[33,35] It was shown by Abakumov and Yassievich[36,37] that at least for the potential $eU = e^2/4\pi\varepsilon_0\varepsilon r$, at a point defect this simple approach gives a result surprisingly close to the result of exact calculations.

The analysis of Eq. (8) shows that for the practically interesting region $3 > kT/(\beta N_{tot}) > 0.1$ the distance L_T corresponding to condition $eU(L_T) = kT$ can be approximated by $L_T \approx 0.71 L_{SCR} \exp[-1.08 kT/(\beta N_{tot})]$. To lose the energy of about kT, the holes need $n_E \approx kT/(m_h s^2 E)^{1/2}$ phonon scattering events and a time of about $n_E \tau_{ph}$, where $\tau_{ph} \approx D_{ph} m_h/(kT)$ and $D_{ph} = \mu_{h-ph} kT/e$. Moving at a velocity $v \approx (2E/m_h)^{1/2}$ a hole thus needs a path $\lambda_E \approx n_E \tau_{ph} v \approx (1.4 D_{ph}/s)$ to lose the energy of about kT. Note that the length λ_E does not depend on energy. Therefore, the capture radius L_C can be estimated as

$$L_C \approx L_T(\gamma L_T/\lambda_E)$$
$$\approx 0.36 \gamma s L_{SCR}^2 \exp(-2.16 kT/(\beta N_{tot}))/D_{ph}. \quad (17)$$

Here, γL_T is the average length of the hole trajectory inside the cylinder with radius L_T. The geometrical factor γ can be calculated by numerical Monte Carlo calculations averaging over all possible trajectories within $L < L_T$ in a potential $eU(L)$ given by Eq. (8). The value of γ slightly depends on the mean free path of holes λ_0. Calculations give $\gamma \approx 2.4$ for $\lambda_0 \gg L_T$, $\gamma \approx 2.8$ for $\lambda_0 \approx L_T$ and $\gamma \approx 3.5$ for $\lambda_0 = 0.1 L_T$. We have used some average value $\gamma \approx 3$ in our calculations. Note that when the length λ_E becomes smaller than γL_T, Eq. 17 cannot be used and one should set $L_C = L_T$.

To get an idea what values of capture parameters A_e and A_h in Eqs. 14 and 15 for transitions between 1D bands and deep levels can be considered as physically reasonable, it is convenient to scale them in the following way:

$$A_h = \alpha \sigma_h/(\pi r_{Dh}^2) \quad (18)$$

and

$$A_e = \alpha \sigma_0/(\pi r_{De}^2). \quad (19)$$

Here, α is a new dimensionless fit parameter, instead of A_h and A_e, and r_{Dh} and r_{De} are radii of wave functions of holes and electrons in 1D bands, respectively, for which we assume $r_{De} \approx r_{Dh} \approx 2$ nm. The expression for capture of electrons from the 1D shallow band by deep levels then resembles the capture of free electrons with effective local concentration $(n_{De}/\pi r_{De}^2)$ multiplied by the unknown fit parameter α. The same holds for holes. The parameter α may be considered as a measure for the overlap between the electronic wave functions of the deep acceptor with those of D_e and D_h.

Finally, we are left with the values of N_M, α, σ_e, σ_h, and E_M as fit parameters. They depend on the type and spatial location of impurity atoms decorating the dislocation.

IV. RESULTS

A. Qualitative characteristics

The effect that metallic impurities or core defects have on the recombination rate between the shallow dislocation bands D_e and D_h, is described in our model by three parameters: α, E_M, and N_M. Figures 3 and 4 illustrate that by the
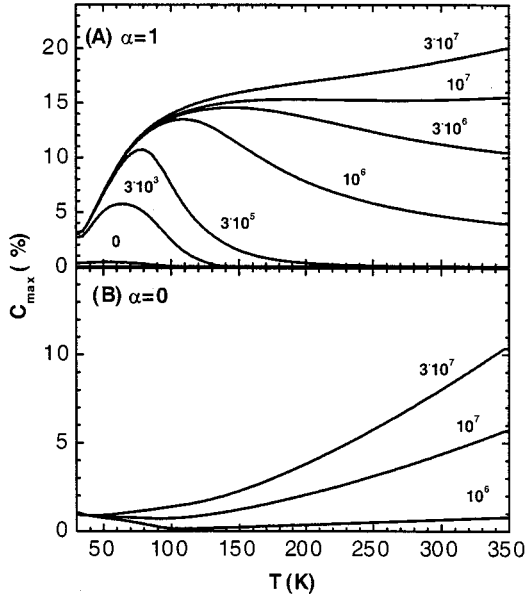
FIG. 3. The EBIC contrast $C_{max}(T)$ calculated for different concentrations N_M from 0 to 3×10^7 cm^{-1} of deep level impurities at the dislocation. Concentrations N_M are shown for each curve. Curves in (A) are calculated for $\alpha=1$, while curves (B) correspond to $\alpha=0$, which means that the transitions between 1D bands and deep levels were neglected. The values of other parameters are $N_d = 10^{15}$ cm^{-3}, $p = 10^{13}$ cm^{-3}, $\sigma_h = 10^{-14}$ cm^2, $\sigma_e = 2 \times 10^{-15}$ cm^2, $E_C - E_M = 0.5$ eV.
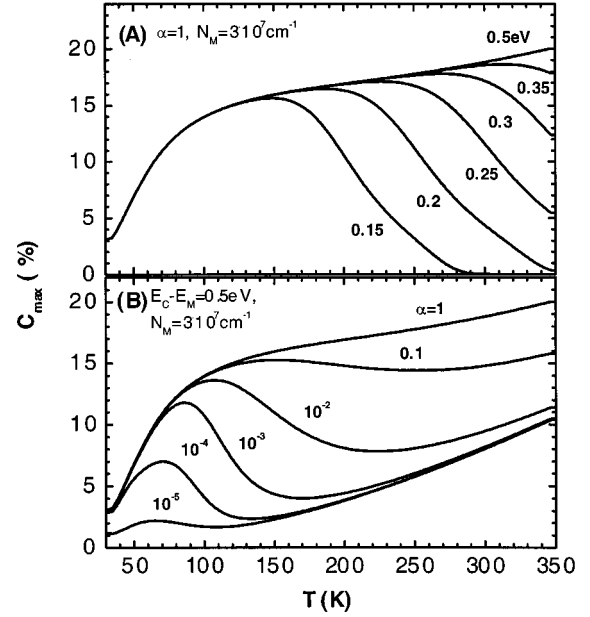

FIG. 4. (A) $C_{max}(T)$ calculated for $\alpha=1$ and different values of $E_C - E_M$, shown for each curve. Other parameters are $N_d = 10^{15}$ cm^{-3}, $p = 10^{13}$ cm^{-3}, $\sigma_h = 10^{-14}$ cm^2, $\sigma_e = 2 \times 10^{-15}$ cm^2, and $N_M = 3 \times 10^7$ cm^{-1}. (B) The EBIC contrast $C_{max}(T)$ calculated for $E_C - E_M = 0.5$ eV and different values of the parameter α from 10^{-5} to 1. Values of α are shown for each curve.

variation of two of these parameters, α and N_M, the experimentally well-established characteristics of $C_{disl}(T)$ are reproduced.

Figure 3 demonstrates that the transitions between deep levels and shallow dislocation bands can strongly affect the EBIC contrast $C_{disl}(T)$. Curves in Fig. 3(A) are calculated for $\alpha=1$, while curves in Fig. 3(B) are calculated neglecting these transitions ($\alpha=0$). Comparison of Fig. 3(A) with experimental $C_{disl}(T)$ data in Fig. 1 shows that our model explains, at least qualitatively, the experimentally observed evolution of $C_{disl}(T)$ dependences with increasing concentration N_M of deep centers at dislocations.

The variations of $C_{disl}(T)$ depending on the value of α are shown in Fig. 4(B) for a strongly decorated dislocation with $N_M = 3 \times 10^7$ cm^{-1}. As one can see, even for quite a small overlap of deep electronic states with 1D bands, when $\alpha \ll 1$, the capture of carriers from 1D bands to the deep impurity level can still give a significant contribution to the recombination.

At the same time, $C_{disl}(T)$ is not sensitive to the energy level of deep acceptors as long, as $E_C - E_M > 0.35$ eV and $T < 300$ K. This is illustrated by Fig. 4(A) that shows $C_{disl}(T)$ calculated for different values of $E_C - E_M$. It also makes intelligible why the experimentally observed $C_{disl}(T)$ are qualitatively the same for different metals, decorating dislocations.

All curves in Figs. 3 and 4 were calculated for some reasonable, but arbitrary values of impurity capture cross sections for electrons $\sigma_e = 2 \times 10^{-15}$ cm^2 and for holes σ_h

$= 10^{-14}$ cm^2. σ_h was chosen larger than σ_e because it corresponds to the capture of a hole by the negatively charged atom, while σ_e corresponds to the capture of an electron by a neutral atom.

B. Fit to experimental data

To check the model, a fit to experimental data was performed using values of N_M, α, σ_h, and σ_e as fit parameters. Since the distance between the Schottky contact and the dislocation is usually not well known, we need one more fit parameter $A = C/C_{max} \leq 1$ to scale the absolute value of calculated contrast C_{max} to the experimentally observed one: $C_{disl}(T) = A \times C_{max}(T)$. However, in most cases we can expect that A should be of the order of one since the experimental conditions are usually adjusted to arrive at optimal imaging.

The parameters N_M, α, σ_h, and σ_e cannot always be independently determined by a fit. From Fig. 3, one sees that for small concentrations of deep acceptors N_M the direct capture of free carriers by impurities gives a very small contribution to the total recombination and then only the value of N_M and the products $\alpha\sigma_h$ and $\alpha\sigma_e$ are obtained from a fit. When N_M becomes larger, all processes yield a contribution to recombination and all parameters may be determined separately. However, when N_M becomes large ($N_M > (1-3) \times 10^6$ cm^{-1}), the number of electrons n_M captured by impurity atoms is mainly limited by the Coulomb interaction and not by N_M. Then $n_M/N_M \ll 1$, and only the value of α and the products $N_M\sigma_e$ and $N_M\sigma_h$ are fixed by the fit.
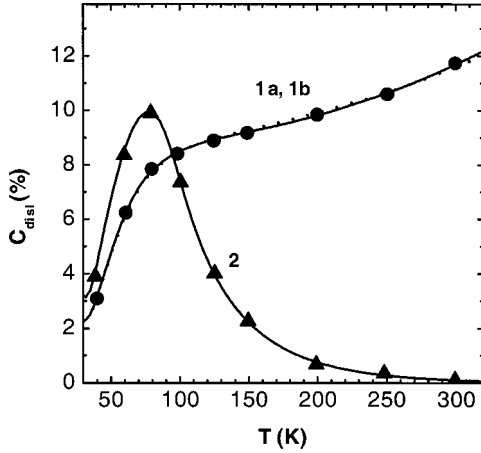
FIG. 5. Points are the experimental data $C_{disl}(T)$ measured for plastically deformed FZ-Si[8] before (curve 1) and after (curve 2) phosphorus diffusion gettering. Solid and dotted lines are calculated using our model. The values of parameters used for calculations are listed in Table I.

In Fig. 5(A), experimental $C_{disl}(T)$ data, marked by points, are shown. They have been obtained for 60° dislocations in the floating zone (FZ) Si[8] lying parallel to the surface of the sample. The sample was plastically deformed by bending at 750 °C for 6 h. The dislocation density is about $(4-8)\times10^5$ cm^{-2}. Curve 1 corresponds to the as-deformed sample, while curve 2 was measured on the same sample after phosphorus diffusion gettering (PDG). The solid and dashed curves represent the fit of our model to these data.

The values of the parameters obtained from the fit are listed in Table I. For curve 2, measured after PDG, it was possible to determine the values of all parameters N_M, α, σ_e, and σ_h. After PDG, the concentration of deep centers is found to be quite small, $N_M\approx2\times10^5$ cm^{-1}, which means a significant reduction compared to the value before PDG.

A good fit to $C_{disl}(T)$ data measured before PDG is obtained only assuming $N_M>2\times10^6$ cm^{-1}. In this case, the occupation of deep acceptor states by electrons is quite small, $n_M/N_M\ll1$ in the whole temperature range. This can be seen in Fig. 7(B) which shows the occupation n_M of deep level by electrons. As mentioned above, the value of N_M, obtained from a fit, becomes now strongly dependent on σ_e and a fit of almost the same quality can be obtained for different combinations of σ_e and N_M.

Assuming that dislocations before and after gettering are decorated by the same impurity in the same state, we can use the value of $\sigma_e=2\times10^{-15}$ cm^2 obtained from the fit to curve 2 also for the fit to curve 1. With this assumption, the fit to curve 1 gives a very large concentration of impurity atoms of $N_M\approx3\times10^7$ cm^{-1} before PDG (see set ''a'' in Table I).

Alternatively, we may start with the assumption that the impurity atoms at such high concentrations already form nanoscale precipitates at the dislocation core. If the density of such nanoscale precipitates is larger than 10^6 cm^{-1}, we can still use our model, because no more than one electron will be captured by each precipitate particle due to a Coulomb blockade. Then we consider each particle as just one deep center, but the effective capture cross section σ_e are expected to be now much larger than for a single atom.

The minimal number of precipitates that still gives a good fit is $N_M\approx2.5\times10^6$ cm^{-1} but they are associated with a significantly larger capture cross section of $\sigma_e\approx5\times10^{-14}$ cm^2 (see set ''b'' in Table I). Therefore, in the case of large contamination of dislocations, the fit of our model to the experimental data yields minimal concentrations of deep centers N_M and the possible combinations of N_M and σ_e, σ_h values.

It is experimentally well established that the EBIC contrast of dislocations depends strongly on the electron beam current I_{beam}, which is related to the minority carriers concentration p. This is consistent with our model that also predicts a strong dependence of contrast on p, since the Coulomb band bending eU_C is sensitively dependent on the minority carrier concentration. The simultaneous fit to $C_{disl}(T)$ and $C_{disl}(I_{beam})$ for the same dislocation would be a critical check of our model.

There are only a few reliable experiments of this kind, because measurements of $C_{disl}(T,I_{beam})$ take a long time, resulting in degradation of a Schottky contact. Figure 6 shows the results of the simultaneous fit of one $C_{disl}(T)$ curve and two $C_{disl}(I_{beam})$ curves measured on the same dislocation.[13] Values of parameters obtained by fit are listed in Table I. One can see that the fit reproduces the measured curve quite well and gives reasonable values of parameters. Since the N_M is again larger than $2\cdot10^6$ cm^{-1}, we cannot estimate N_M and σ_e independently, but can only obtain the possible combinations of N_M and σ_e (set ''a'' and ''b'' in Table I). The parameter $A=C_{disl}/C_{max}$ is small, about 0.25,

TABLE I. Values of parameters used for calculation of curves shown in Figs. 5 and 6. The energy level E_C-E_M was assumed to be 0.5 eV, $N_d=5\times10^{14}$ cm^{-3}, $p=10^{13}$ cm^{-3} for Fig. 5 and $p=10^{11}$ I_{beam} (pA) cm^{-3} for Fig. 6. Parameters marked by an * were kept fixed during fit.

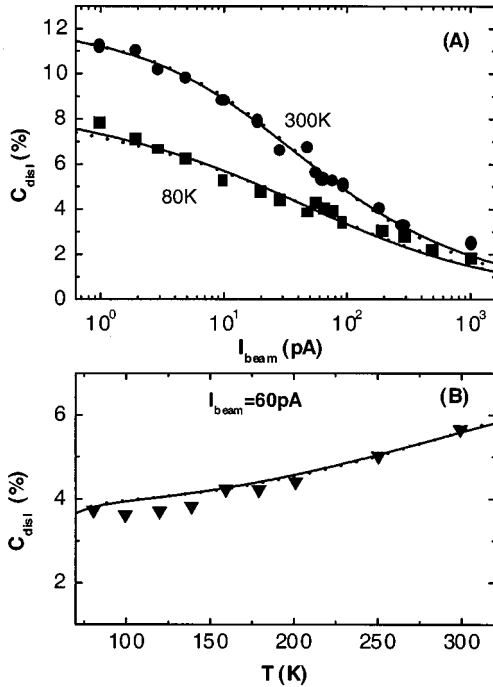| Parameters	N_M (cm^{-1})	α	A	σ_h (10^{-14} cm^2)	σ_e (10^{-15} cm^2)
Fig. 5, curve 2	$(2.2\pm0.3)\times10^5$	0.9 ± 0.1	1.0 ± 0.1	(6.5 ± 0.7)	(2.0 ± 0.5)
Fig. 5, curve 1		0.9 ± 0.2	0.7 ± 0.07		
set ''a''	$(3.0\pm0.5)\times10^7$			(6.5 ± 0.3)	*2
set ''b''	$(2.4\pm0.2)\times10^6$			(5.5 ± 0.5)	*50
Fig. 6		0.9 ± 0.2	0.23 ± 0.03		
set ''a''	$(3.2\pm0.5)\times10^7$			(7.5 ± 1)	*3
set ''b''	$(3.0\pm0.5)\times10^6$			(6 ± 1)	*60

FIG. 6. The experimental dependences of EBIC contrast C_{disl} on electron beam current I_{beam} [points in (A)] and on temperature T [data points (B)] measured for the same dislocation,[13] and the result of their simultaneous fit (solid and dotted lines). The values of parameters used for calculation are listed in Table I.
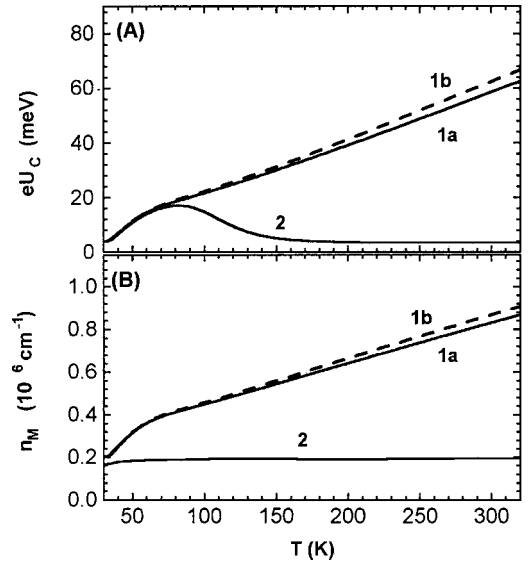

FIG. 7. (A) Coulomb band bending eU_C and (B) number of electrons n_M captured to the deep level calculated for the same parameters as curves 1a, 1b, and 2 in Fig. 5. (B) the occupation n_M of deep level by electrons. Curves 1a and 1b correspond to the combination of parameters, labeled as set ''a'' and ''b'' in Table I.

because the measurements[13] were made on misfit dislocations in a SiGe/Si heterostructure. In this case, the contrast should be smaller than calculated by Donolato's theory[17] due to the valence band bending in the heterostructure interface.

The rigid shift of all states inside the extended core region, as well as the hole capture by the attractive potential of the negatively charged dislocation, have been based on the assumption that the dislocation line charge is sufficiently small to allow for a quasiclassical approach. As outlined in Sec. III B, this assumption implies that electron-hole generation under the conditions of EBIC measurements is sufficiently large so that the concentration of minority carriers is much larger that its thermodynamic equilibrium value. In this case, the dislocation line charge eN_{tot} resulting from the occupation of all dislocation-related states, should become adjusted to quite small values as soon as stationary conditions between generation and recombination of carriers at the dislocation are established, since the capture rate for majority charge carriers decreases exponentially with the increase of eN_{tot}. This is illustrated in Fig. 7(A), which shows that the electrostatic potential calculated for typical EBIC experiments is indeed quite small and our calculations are self consistent. The Coulomb band bending eU_C works as stabilizing negative feedback adjusting the flux of holes to the flux of electrons at dislocations.

Under these conditions many details of a quantum mechanical treatment may be omitted since it gives a correction to the electrostatic potential less or about kT. More than that, a small change of some parameters that couple the potential eU_C with the dislocation charge eN_{tot} will not lead to sig-

nificant changes of the recombination rate, but instead, the dislocation charge will be slightly readjusted, keeping almost the same value of the recombination rate.

We note that in our simplified model, the localization length of electrons and holes in the 1D bands D_e and D_h was assumed to be larger or comparable with the distance $1/N_M$ between the deep centers along the dislocation. For $T > 40$ K and $N_M > 10^5$ cm^{-1}, it is a quite reasonable assumption (see Refs. 23–27). If the temperature is too low ($T < 30$–40 K) and, at the same time, N_M is too small ($N_M < 10^4$–10^5 cm^{-1}) the localization length can become much smaller than $1/N_M$ and the model should be modified to take this into account, for example, by introducing a dependence of parameter α on T and N_M.

V. DISCUSSION AND SUMMARY

A. Previous recombination models

Basic features concerning the action of dislocations on charge carrier recombination have been investigated and modeled in the 1960s and 1970s. They have been mainly derived from experimental results of the charge-carrier lifetime, stationary photo conductivity, and the Hall effect of plastically deformed germanium, and later from EBIC data of dislocations in silicon.

In the recombination model of dislocations, Morrison[46] and later, Figielski,[47] proposed a classical concept of how a negative line charge of the dislocation affects the capture of electrons and holes. Central points of this model are the repulsive potential barrier for electrons, whose amplitude varies with the dislocation line charge and which affects the capture rate through an exponential factor, and the attractive potential well for holes.

Inconsistencies with independent experimental results in germanium led Schröter[43] to integrate theoretical work by Gulyaev[48] on the tunneling of electrons in the repulsive potential and by Sokolova[40] on the capture of holes into bound hole states. Thereby the capture of holes became a two-stage transition, the first leading from the valence band to the bound hole states, the second from there to the deep states at the dislocation. This model has relieved the inconsistency between the results of photo conductivity and the Hall effect and also explained why two different capture rates of holes had been observed by an appropriate choice of experimental conditions.

Shikin and Shikina[49] and later Labusch and Hess[20] have investigated the combined effect of electrostatic and deformation potential on the conduction-band edge near to a negatively charged dislocation. The corrections of the simple rigid band model, which relates band shifts only to the electrostatic potential, have been found significant. However, many experiments fail to detect these corrections, since the band shifts due to the electrostatic potential and due to the total potential both vary approximately linearly with the dislocation line charge, and those experiments are only sensitive to the total shift. Clear evidence for those corrections has been found by photo-conductance spectroscopy of dislocations in germanium.[20]

First results of the EBIC contrast as a function of temperature for dislocations and stacking faults have been obtained by Kimerling, Leamy, and Patel.[50]

Ourmazd[44] has adapted the model of Schröter[43] to the quantitative analysis of the EBIC contrast, thereby opening the possibility to investigate the electrical properties of single dislocations. He studied $C_{disl}(T)$ ($120\,\mathrm{K} \leqslant T \leqslant 300\,\mathrm{K}$) of various dislocation types in n-type silicon, whose structural properties were known from TEM weak-beam investigations. Under the condition of heavy doping, Ourmazd has arrived at a consistent interpretation in terms of the two-stage hole capture and of considering tunneling only for the heavily charged dislocations. Since the tunneling rate is sensitively dependent on the electron effective mass, which is larger in silicon than in germanium, its contribution in silicon is limited to small ranges of temperature, doping, etc.

Although the treatments of hole capture in the attractive potential of the dislocation in our model and in the model of Ourmazd-Schröter are significantly different, they may be considered as two approaches to the general solution, which is still not known. Our approach describes the capture for small dislocation line charges. With increasing line charge, the shallow 1D band, which splits off from the conduction band, is pushed out of the band gap. At the same time, the properties of the hole band become more and more determined by the electrostatic part of the dislocation potential with the deformation potential as correction. Furthermore, a set of more shallow hole bands appears,[51,31] whose role in

hole capture remained unconsidered in the theoretical treatment of Sokolova and in the model of Ourmazd-Schröter.

Another approach to the hole capture problem has been given by Wilshaw and Booker.[45,52] Their model is built on the assumption that Sokolova's cascade capture by the 1D band associated with bound hole states only operates for holes inside the dislocation space charge region of radius L_{SCR}. The re-emission from the bound hole states to the valence band is neglected and the transition to the bound hole states is assumed to be rate limiting. The model of Wilshaw and Booker has been widely applied to $C_{disl}(T, I_{beam})$ data (Si: 120, ... ,370 K), especially to reproduce for the first time the dependence on the current of the electron probe, I_{beam}. However, a critical experimental or theoretical check of the basic assumptions of the model is missing. It is unclear how the assumption of a huge capture radius L_{SCR} and of negligible re-emission can be made consistent with Sokolova's cascade capture model.

As already mentioned (Sec. III A) the new feature of our model results from C_{disl} data, which were obtained for clean and slightly decorated dislocations and showed a pronounced peak below 120 K. Experimental results in this temperature range were not available and therefore have not been considered in the previous models.

B. Summary

We have developed a model that comprises a statistical description of the electron-hole recombination at dislocations under the conditions of EBIC measurements. We have reduced the number of free parameters by consideration of independent experimental and theoretical results so that the validity of the model could be checked and confirmed by fits to available EBIC data. Like previous ones by Ourmazd[44] and by Wilshaw and Booker,[45] our model establishes the link to phenomenological modeling of EBIC contrast, as given in a series of papers by Donolato and by Pasemann (see Ref. 17). As a different aspect, our model includes the interaction between metallic impurities or core defects and dislocation energy bands. We have demonstrated that it is this interaction that accounts for the basic characteristics of the EBIC contrast as a function of temperature, beam current, and metallic impurity concentration. Combined with EBIC investigations of samples with well controlled contamination and extended to higher temperatures, our model opens a quantitative access to segregation and electronic structure of metallic impurities at dislocations.

ACKNOWLEDGMENTS

---

*Permanent address: Institute of Solid State Physics, 142432, Chernogolovka, Moscow Distr., Russia. Corresponding author Prof. Vitaly Kveder; email address: kveder@issp.ac.ru; FAX: (007 096) 576-41-11.

[1] T. Heiser and E. R. Weber, Phys. Rev. B **58**, 3893 (1998).

[2] D. Gilles, W. Schröter, and W. Bergholz, Phys. Rev. B **41**, 5770 (1990).

[3] M. Kittler, C. Ulhaq-Bouillet, and V. Higgs, J. Appl. Phys. **78**,

4573 (1995).

[4] V. Higgs and M. Kittler, Appl. Phys. Lett. **65**, 2804 (1994).

[5] M. Kittler and W. Seifert, Scanning **15**, 316 (1993).

[6] M. Kittler, W. Seifert, and V. Higgs, Phys. Status Solidi A **137**, 327 (1993).

[7] O. Krüger, W. Seifert, M. Kittler, A. Gutjahr, M. Konuma, K. Said, and J. Poortmans, Solid State Phenom. **63−64**, 509 (1998).

[8] K. Knobloch, M. Kittler, W. Seifert, J. J. Simon, and I. Perichaud, Solid State Phenom. **63−64**, 105 (1998).

[9] S. Kusanagi, T. Sekiguchi, B. Shen, and K. Sumino, Mater. Sci. Technol. **11**, 685 (1995).

[10] B. Shen, T. Sekiguchi, and K. Sumino, Jpn. J. Appl. Phys. **35**, 3301 (1996).

[11] M. Kittler and W. Seifert, Phys. Status Solidi A **150**, 463 (1995).

[12] M. Kittler, J. Lärz, W. Seifert, M. Seibt, and W. Schröter, Appl. Phys. Lett. **58**, 911 (1991).

[13] M. Kittler and W. Seifert, Mater. Sci. Eng., B **24**, 78 (1994).

[14] M. Kittler, C. Ulhaq-Bouillet, and V. Higgs, Mater. Sci. Eng., B **24**, 52 (1994).

[15] M. Kittler, C. Ulhaq-Bouillet, and V. Higgs, Mater. Sci. Forum **196−201**, 383 (1995).

[16] W. Seifert, K. Knobloch, and M. Kittler, Solid State Phenom. **57−58**, 287 (1997).

[17] C. Donolato in *Point and Extended Defects in Semiconductors*, edited by G. Benedek, A. Cavallini, and W. Schröter (Plenum New York, 1989) p. 225.

[18] M. Kittler and W. Seifert, Mater. Sci. Forum **196−201**, 1123 (1995).

[19] H. Alexander and H. Teichler, *Dislocations in: Handbook of Semiconductor Technology*, edited by K. A. Jackson and W. Schröter (Wiley-VCH, New York, 2000), Vol. 1, p. 291.

[20] R. Labusch and J. Hess, Phys. Status Solidi A **146**, 145 (1994).

[21] V. V. Kveder, Yu. A. Ossipyan, I. R. Sagdeev, A. I. Shalynin, and M. N. Zolotukhin, Phys. Status Solidi A **87**, 657 (1985).

[22] M. Brohl and H. Alexander, Inst. Phys. Conf. Ser. **104**, 163 (1989).

[23] M. Brohl, M. D. Dressel, H. W. Helberg, and H. Alexander, Philos. Mag. B **61**, 97 (1990).

[24] V. Kveder, T. Sekiguchi, and K. Sumino, Phys. Rev. B **51**, 16 721 (1995).

[25] Y. Lelikov, Y. Rebane, S. Ruvimov, D. Tarbin, A. Sitnikova, and Y. Shreter, Phys. Status Solidi B **172**, 53 (1992).

[26] V. V. Kveder, E. A. Steinman, and H. G. Grimmeiss, Solid State Phenom. **47−48**, 419 (1996).

[27] V. V. Kveder, E. A. Steinman, S. A. Shevchenko, and H. G. Grimmeiss, Phys. Rev. B **51**, 10 520 (1995).

[28] J. L. Farvacque, Mater. Sci. Eng., B **42**, 110 (1996).

[29] Landolt-Börnstein, New Series Vol. 41 B, edited by O. Madelung, U. Rössler, and M. Schulz (Springer-Verlag, Berlin, 1999).

[30] *Properties of Crystalline Silicon*, edited by R. Hull, EMIS Datareviews Series No. 20 (INSPEC, England, 1999).

[31] W. Schröter, J. Kronewitz, U. Gnauert, F. Riedel, and M. Seibt, Phys. Rev. B **52**, 13 726 (1995).

[32] W. T. Read, Philos. Mag. **45**, 775 (1954).

[33] J. J. Thomson, Philos. Mag. **47**, 337 (1924).

[34] L. P. Pitayevskii, Zh. Eksp. Teor. Fiz. **42**, 1326 (1962) [Sov. Phys. JETP **15**, 919 (1962)].

[35] M. Lax, Phys. Rev. **119**, 1502 (1960).

[36] V. A. Abakumov and I. N. Yassievich, Zh. Eksp. Teor. Fiz. **71**, 657 1976 [Sov. Phys. JETP **44**, 345 (1976)].

[37] I. N. Yassievich, in *Semiconductor Physics*, edited by V. M. Tuchkevich and V. Ya. Frenkel (Consultants Bureau, New York, 1986) p. 519.

[38] Y. T. Rebane and Y. G. Shreter, Phys. Status Solidi A **137**, 603 (1993).

[39] Y. T. Rebane and J. W. Steeds, Phys. Rev. B **48**, 14 963 (1993).

[40] E. B. Sokolova, Fiz. Tekh. Poluprovodn. **3**, 1512 1969 [Sov. Phys. Semicond. **3**, 1266 (1969)].

[41] G. L. Pearson and J. Bardeen, Phys. Rev. **75**, 865 (1948).

[42] F. J. Morin and J. P. Maita, Phys. Rev. **96**, 28 (1954).

[43] W. Schröter, Phys. Status Solidi A **19**, 159 (1973).

[44] A. Ourmazd, Cryst. Res. Technol. **16**, 137 (1981).

[45] P. R. Wilshaw and G. R. Booker, Inst. Phys. Conf. Ser. **76**, 329 (1985).

[46] S. R. Morrison, Phys. Rev. **104**, 619 (1956).

[47] T. Figielski, Solid-State Electron. **21**, 1403 (1978).

[48] Yu. V. Gulyaev, Fiz. Tverd. Tela (Leningrad) **4**, 1285 (1962) [Sov. Phys. Solid State **4**, 941 (1962)].

[49] V. B. Shikin and N. I. Shikina, Phys. Status Solidi A **108**, 669 (1988).

[50] L. C. Kimerling, H. J. Leamy, and J. R. Patel, Appl. Phys. Lett. **30**, 217 (1977).

[51] V. L. Bonch-Bruevich and V. B. Glasko Fiz. Tverd. Tela (Leningrad) **3**, 36 (1961) [Sov. Phys. Solid State **3**, 26 (1961)].

[52] P. R. Wilshaw, T. S. Fell, and G. R. Booker in *Point and Extended Defects in Semiconductors*, edited by G. Benedek, A. Cavallini, and W. Schröter (Plenum, New York, 1989), p. 243.